

# Variational quantum eigensolver for chemical molecules

Luca Ion and Adam Smith  
*School of Physics & Astronomy, University of Nottingham, Nottingham, UK*  
(Dated: May 16, 2023)

Solving multi-particle systems is an important topic in quantum chemistry and condensed matter physics. In this article, we focus on finding the ground states and ground-state energies for the  $\text{He-H}^+$  and  $\text{H}_2\text{O}$  molecules using quantum computing. We employ the variational quantum eigensolver (VQE), which is executed both on a quantum computer simulator and on an IBM quantum device. We compare the results against the exact ground-state energy obtained through classical methods. The  $\text{H}_2\text{O}$  simulations were run on Nottingham's High Performance Computer (HPC).

## I. INTRODUCTION

The second quantum revolution [1] gave rise to the fields of quantum information and quantum computation. At present, we find ourselves in the era of Noisy Intermediate-Scale Quantum (NISQ) [2] devices, meaning that quantum devices are built from a few hundred qubits and suffer from qubit errors (noise). Nevertheless, this era has provided new technologies and disciplines such as quantum cryptography [3] and quantum machine learning [4].

An important field that benefits from quantum computation is the quantum chemistry of molecules. The reason is that the Hilbert space grows exponentially with the number of qubits  $N$ , and therefore complex molecules comprising many particles require substantial resources to store and manipulate on a classical computer using classical methods. In contrast, quantum computation allows us to work with quantum circuits and quantum gates, which can simplify the process.

In this work, we focus on the VQE algorithm used to find the ground state and ground-state energy of a multi-particle Hamiltonian. We first consider the  $\text{He-H}^+$  molecule, which was studied extensively in [5]. We introduce the circuit ansatz and discuss how the ansatz differs when a deeper circuit structure is desired. We then discuss the results of VQE optimization. Finally, we study the more complex  $\text{H}_2\text{O}$  molecule to assess how VQE performs for a larger system.

## II. EXACT DIAGONALIZATION

First, to find the ground-state energy for the Hamiltonian associated with the molecule under inspection, one can use an eigenvalue decomposition. The method used to obtain the Hamiltonians for various molecules is discussed in Sec. III. Once the Hamiltonian  $H$  is known, one can use classical methods to find the ground-state energy. We used NumPy for all mathematical operations, including eigenvalue decomposition and the computation of the exact ground-state energy.

## III. FINDING THE HAMILTONIAN

The first step is to obtain the Hamiltonian for the molecule under inspection. For  $\text{He-H}^+$ , we use the

Hamiltonian studied in [5]; this is a two-qubit Hamiltonian and is shown in Sec. VI. For more complex molecules, such as  $\text{H}_2\text{O}$ , we use the built-in PennyLane `molecularHamiltonian` method [6].

## IV. QUANTUM CIRCUIT ANSATZ

The main goal is to carry out optimization on a quantum circuit to obtain a state that approximates the ground state of the Hamiltonian in question. The first task is to construct a quantum circuit structure that is able to approximate the ground state. The circuit structure used in this paper can be extended over multiple layers  $M$  and multiple qubits  $N$ . The circuit in Fig. 1 is an example of such a structure. The symbols  $R_X$  and  $R_Z$  denote single-qubit rotation gates,

$$R_X(\theta_a) = \exp\left(-i\frac{\theta_a}{2}X\right), \quad (1)$$

$$R_Z(\theta_b) = \exp\left(-i\frac{\theta_b}{2}Z\right), \quad (2)$$

where  $X$  and  $Z$  are Pauli operators and  $\theta_a, \theta_b$  are rotation angles. Note that each rotation gate takes an angle as an argument. The full set of such angles constitutes the parameters to be optimized so that the output state approximates the ground state.

In addition, we require entangling operations to make individual qubits “communicate”; this is achieved using the  $CZ$  (Control-Z) gate, a two-qubit gate with the first qubit as the control and the second as the target. In matrix form,

$$CZ = \begin{pmatrix} 1 & 0 & 0 & 0 \\ 0 & 1 & 0 & 0 \\ 0 & 0 & 1 & 0 \\ 0 & 0 & 0 & -1 \end{pmatrix}. \quad (3)$$

The  $CZ$  gate applies the  $Z$  operation to the target qubit if the control qubit is  $|1\rangle$ , and acts trivially otherwise. In Fig. 1, all connections between wires are  $CZ$  gates.

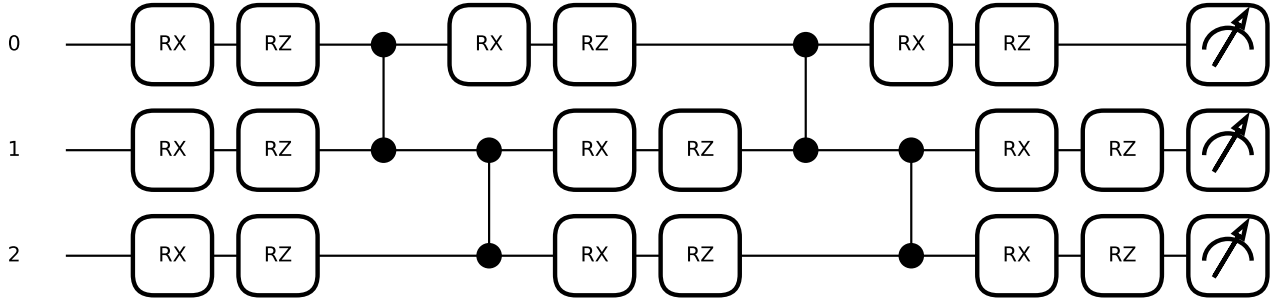


FIG. 1. Circuit ansatz for  $N = 3$  and  $M = 2$ .  $R_X$  and  $R_Z$  are rotation gates and the connection between the wires is done through Control-Z gates.

## V. METHOD

In order to approximate the ground-state energy, we employ the VQE algorithm. The ansatz circuit is optimized such that the state produced by the circuit  $|\psi\rangle$  minimizes the energy

$$E = \langle \psi | H | \psi \rangle. \quad (4)$$

It is important to note that  $|\psi\rangle$  and, as a result,  $E$  depend on the parameter list  $\vec{\theta}$ ; in machine learning language,  $E$  is the loss function. The optimization method used here is gradient descent [7] and variations of it. For classical gradient descent, the parameter list is updated over multiple iterations according to

$$\vec{\theta}_{n+1} = \vec{\theta}_n - \eta \nabla E(\vec{\theta}_n), \quad (5)$$

where  $\eta$  is the learning rate. To approximate the gradient, multiple methods can be used. In this paper, we compare the following gradient descent approximation schemes: first order finite difference (FOGD) [8], second order finite difference (SOGD) [8], simultaneous perturbation stochastic approximation (SPSA) [9], and parameter shift (PS) [10].

Choosing a tuning method for  $\eta$  is not an easy task; here a constant  $\eta$  is used for FOGD, SOGD, and PS, and a decaying  $\eta$  is used for SPSA. Other tuning methods may be used [11]. The number of parameters to optimize depends on the number of qubits  $N$  and the number of layers in the circuit ansatz  $M$  according to

$$\text{parameters} = 2N(M + 1). \quad (6)$$

Parameters are initialized randomly, with each parameter initialized to  $2\pi$  times a random number between 0 and 1. The number of optimization iterations is fixed, although a stopping criterion could also be implemented. Finally, the number of circuit evaluations (shots) is set to 8192.

## VI. HE-H<sup>+</sup> RESULTS

The first molecule considered is He-H<sup>+</sup> (helium hydride). This molecule's Hamiltonian depends on the dis-

tance between the atoms  $R$ . The Hamiltonian is a two-qubit Hamiltonian given by

$$H = \frac{1}{2} [J_x(X1 + 1X) + J_z(Z1 + 1Z) + J_{xx}XX + J_{zz}ZZ + J_{xz}(XZ + ZX) + C] \quad (7)$$

where  $J_x$ ,  $J_z$ ,  $J_{xx}$ ,  $J_{zz}$ , and  $C$  are parameters dependent on  $R$ .

For this molecule, we use  $\eta = 0.8$  and 20 iterations in the optimization. The optimization plots for each method are shown in Fig. 2. The best convergence is observed for the parameter-shift and SOGD methods. SPSA decreases rapidly in the first few iterations but then stagnates. These observations depend on the tuning of  $\eta$ , and selecting an appropriate learning rate is therefore an important task.

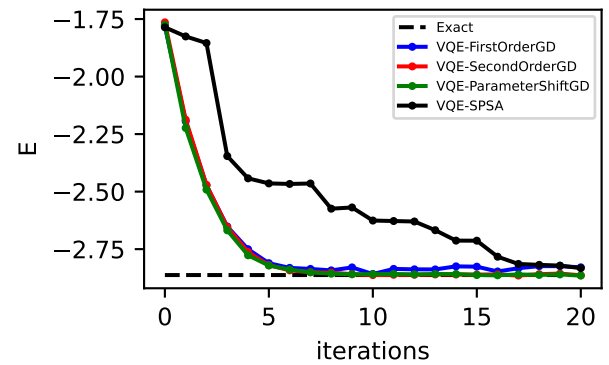


FIG. 2. Simulated He-H<sup>+</sup> optimization for  $R = 0.9\text{\AA}$ ,  $M = 1$ ,  $N = 2$ ,  $\eta = 0.8$  and for all the different gradient descent variants.

Additionally, optimization can be carried out for different ansatz depths  $M$  and the final energies compared. For this molecule,  $M = 1$  is sufficient for convergence, so increasing  $M$  does not yield substantially better approximations.

To run the optimization on a real IBM machine, it is impractical to evaluate all methods due to long queue

times; therefore, SOGD was used since it performed well in simulation. Figure 3 shows the optimization results. The final energy does not match the exact energy closely, which reflects the noisy nature of current quantum hardware.

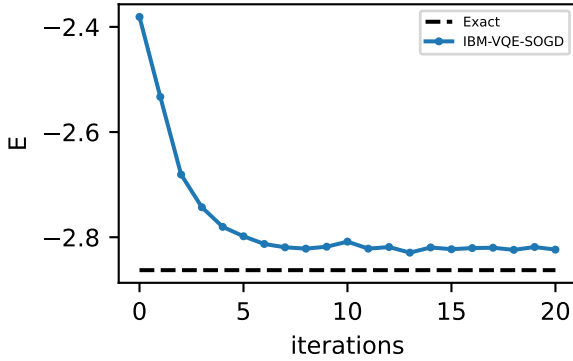


FIG. 3. IBM He-H<sup>+</sup> optimization for  $R = 0.9\text{\AA}$ ,  $M = 1$ ,  $N = 2$ ,  $\eta = 0.8$  and SOGD.

The optimization was also carried out for  $R = 0.75\text{\AA}$  and  $R = 1.05\text{\AA}$  on the real IBM machine and was run in simulation for every  $R \in [0.5, 2.5]$  with step size 0.05. In Fig. 4, the approximated energy is plotted for each  $R$  and compared against the exact energy obtained through exact diagonalization. The energy curve has a minimum at  $R = 0.9\text{\AA}$ , which motivates our choice of this value for the other plots in this section.

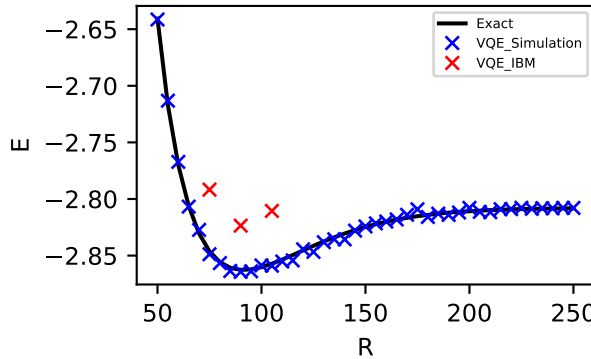


FIG. 4. He-H<sup>+</sup>: Energy( $E$ ) against  $R$  in picometres plot for the exact, VQE-simulation (SOGD), and IBM results using  $M = 1$  ansatz and  $\eta = 0.8$ .

## VII. H<sub>2</sub>O RESULTS

The next molecule considered is water, H<sub>2</sub>O. We consider a simplified model [12] where the active orbitals and active electrons are both set to 4. With these constraints, PennyLane returns an eight-qubit Hamiltonian

for this system; without limiting the active orbitals, a fourteen-qubit Hamiltonian is obtained. Since this system is significantly larger than the He-H<sup>+</sup> system, the optimization takes considerably longer to complete, even for a  $M = 1$  ansatz. As a result, the HPC was used to benefit from parallelism.

The water molecule requires two parameters to describe its geometry:  $R$  and  $\phi$ , where  $R$  is the O-H bond length and  $\phi$  is the H-O-H angle, as shown in Fig. 5. Different values of these parameters produce different Hamiltonians and thus different ground-state energies. When examining the Hamiltonians returned by PennyLane, we found that the lowest ground-state energy occurs for  $R = 1.9\text{\AA}$  and  $\phi = 1.75$  rad. This differs from typical literature values ( $R = 0.96\text{\AA}$  and  $\phi = 1.8$  rad) due to the approximations introduced by limiting the active orbitals and active electrons.

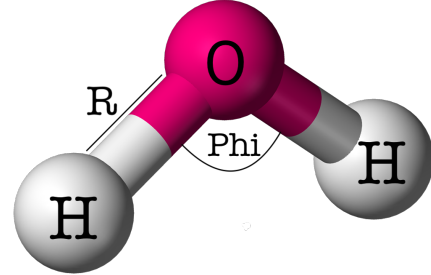


FIG. 5. The geometry of the H<sub>2</sub>O molecule.  $R$  is the O-H bond length and  $\phi$  is the HOH angle.

Optimization was run for  $M = 1, 2, 3, 4, 5, 8$  layered ansatz circuits for 100 iterations with  $\eta = 0.8$ . It was generally found that even a  $M = 1$  ansatz produces good approximations. Figure 6 shows the optimization for each method. All methods converge successfully except SPSA, which likely requires improved tuning beyond a simple decay schedule.

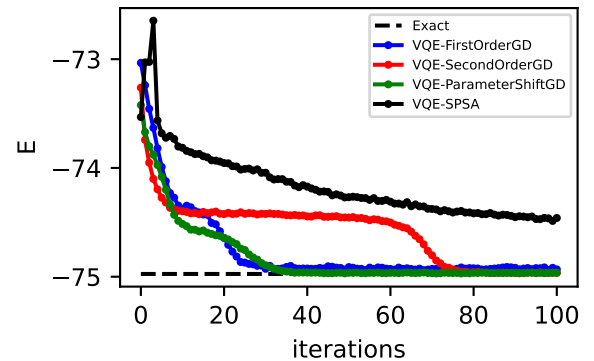


FIG. 6. Simulated H<sub>2</sub>O optimization for  $\phi = 1.75$  rad,  $R = 1.9\text{\AA}$ ,  $M = 1$ ,  $N = 8$ ,  $\eta = 0.8$  and for all the different gradient descent variants.

To show the dependence of the ground-state energy

on the angle  $\phi$ , the bond length is fixed to  $R = 1.9\text{\AA}$  and the angle is varied from  $5^\circ$  to  $180^\circ$  in  $5^\circ$  increments. Optimization is then run for each angle and both the exact energy and the approximated energy are plotted. By running optimization multiple times, it was observed that the PS method generally performed best; therefore, it is used here. Figure 7 shows the results for  $M = 1, 2, 3$  ansatz circuits. A dip in the energy at  $\phi = 1.75$  rad is observed, analogous to the minimum seen for He-H<sup>+</sup> in Fig. 4. For some values of  $\phi$ , optimization becomes trapped and does not converge within the allotted number of sweeps. Addressing this likely requires improved learning-rate tuning and longer, repeated optimizations.

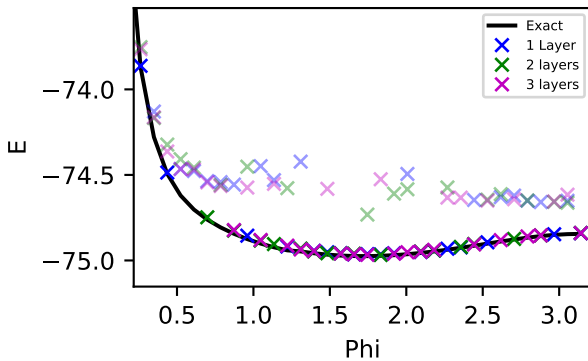


FIG. 7. H<sub>2</sub>O: Energy( $E$ ) against  $\phi$  plot for the exact and VQE-simulation (PS) results using  $M = 1, 2, 3$  layered ansatz and  $\eta = 0.8$ . The more transparent data corresponds to instances that did not converge in the optimization.

## VIII. DISCUSSION

In this work, we carried out VQE for He-H<sup>+</sup> and H<sub>2</sub>O using different ansatz circuits and multiple gradient descent methods. We find that VQE can successfully approximate the ground-state energy even for a complex molecule such as H<sub>2</sub>O. For the simpler He-H<sup>+</sup> molecule, the algorithm was also performed on a real IBM machine,

highlighting the noisy nature of current quantum devices in the optimization results.

From the optimization plots, we observe that PS generally performs best, while SPSA performs worst under the settings considered. PS has the advantage of computing an exact gradient, whereas SPSA has an intrinsically stochastic character. On the other hand, SPSA can be faster in terms of required circuit calls, as it uses considerably fewer circuit evaluations than the other methods. For He-H<sup>+</sup> this speed-up is not pronounced due to the small circuit size, but for H<sub>2</sub>O the difference is substantial. Moreover, SPSA is often favoured on real IBM devices because each circuit evaluation incurs queueing time; fewer circuit calls can therefore reduce total wall-clock time. However, SPSA introduces additional hyperparameters, and the challenge of tuning them is correspondingly greater.

Further investigation is needed for the H<sub>2</sub>O molecule. First, improved hyperparameter tuning and repeated optimization runs may increase convergence across more of the points in Fig. 7. Another modification is to change the initialization strategy for the ansatz. Instead of fully random rotations, one can initialize to small rotations  $\vec{\theta}_0 \approx \vec{0}$ , so that the initial output state is close to a computational basis state and therefore exhibits low entanglement. This is motivated by the possibility that the true ground state also has relatively low entanglement, making convergence easier. Next, it would be interesting to keep  $\phi$  fixed and vary  $R$  to obtain the energy as a function of bond length. Finally, increasing the active-orbital space to obtain a more realistic H<sub>2</sub>O model (which will increase  $N$ ) and performing optimization for that larger instance would be a natural next step.

## IX. ACKNOWLEDGMENTS AND COMMENTS

I would like to thank my supervisor for their guidance and support throughout this mini-project, as well as the University of Nottingham for providing access to high-performance computing (HPC) resources. This work was carried out as part of my MSc degree and is intended as a learning exercise rather than a contribution of novel research.

---

[1] J. P. Dowling and G. J. Milburn, Quantum technology: The second quantum revolution (2002).

[2] J. Preskill, Quantum Computing in the NISQ era and beyond, *Quantum* 2, 79 (2018).

[3] D. J. Bernstein, J. Buchmann, and E. Dahmén, Post-quantum cryptography (Springer, 2009).

[4] X. Gao, Z. Zhang, and L. Duan, An efficient quantum algorithm for generative machine learning (2017).

[5] A. Peruzzo, J. McClean, P. Shadbolt, M.-H. Yung, X.-Q. Zhou, P. J. Love, A. Aspuru-Guzik, and J. L. O'Brien, A variational eigenvalue solver on a photonic quantum processor, *Nature Communications* 5, 10.1038/ncomms5213 (2014).

[6] V. Bergholm, J. Izaac, M. Schuld, C. Gogolin, S. Ahmed, V. Ajith, M. S. Alam, G. Alonso-Linaje, B. Akash-Narayanan, A. Asadi, J. M. Arrazola, U. Azad, S. Banning, C. Blank, T. R. Bromley, B. A. Cordier, J. Ceroni, A. Delgado, O. D. Matteo, A. Dusko, T. Garg, D. Guala, A. Hayes, R. Hill, A. Ijaz, T. Isacsson, D. Ittah, S. Jahanjiri, P. Jain, E. Jiang, A. Khandelwal, K. Kottmann, R. A. Lang, C. Lee, T. Loke, A. Lowe, K. McKiernan, J. Meyer, J. A. Montañez-Barrera, R. Moyard, Z. Niu,

L. J. O’Riordan, S. Oud, A. Panigrahi, C.-Y. Park, D. Polatajko, N. Quesada, C. Roberts, N. Sá, I. Schoch, B. Shi, S. Shu, S. Sim, A. Singh, I. Strandberg, J. Soni, A. Száva, S. Thabet, R. A. Vargas-Hernández, T. Vincent, N. Vitucci, M. Weber, D. Wierichs, R. Wiersema, M. Willmann, V. Wong, S. Zhang, and N. Killoran, PennyLane: Automatic differentiation of hybrid quantum-classical computations (2022), arXiv:1811.04968 [quant-ph].

[7] C. Lemaréchal, Cauchy and the gradient method, Optimization Stories, 251–254 (2012).

[8] S. Venkateshan and P. Swaminathan, Numerical differentiation, in Computational Methods in Engineering (Elsevier, 2014) pp. 295–315.

[9] J. Spall, Multivariate stochastic approximation using a simultaneous perturbation gradient approximation, IEEE Transactions on Automatic Control 37, 332–341 (1992).

[10] PennyLane, Parameter-shift rules (2022).

[11] L. N. Smith, Cyclical learning rates for training neural networks, 2017 IEEE Winter Conference on Applications of Computer Vision (WACV) 10.1109/wacv.2017.58 (2017).

[12] A. Delgado, Building molecular hamiltonians - pennylane (2022).